

Size-Dependent Melting Properties of Small Tin Particles: Nanocalorimetric Measurements

S. L. Lai,¹ J. Y. Guo,¹ V. Petrova,² G. Ramanath,¹ and L. H. Allen¹

¹*Department of Materials Science and Engineering, University of Illinois at Urbana-Champaign, Urbana, Illinois 61801*

²*Center for Microanalysis of Materials, University of Illinois at Urbana-Champaign, Urbana, Illinois 61801*

(Received 10 November 1995)

For the first time, the latent heat of fusion ΔH_m for Sn particles formed by evaporation on inert substrate with radii ranging from 5 to 50 nm has been measured directly using a novel scanning nanocalorimeter. A particle-size-dependent reduction of ΔH_m has been observed. An "excluded volume" is introduced to describe the latent heat of fusion from the enhanced surface melting of small particles. Melting point depression has also been found by our nanocalorimetric technique. [S0031-9007(96)00495-4]

PACS numbers: 61.46.+w, 64.70.Dv, 65.40.+g

The unusual properties of nanometer-sized materials have generated tremendous interest in both scientific and technological communities [1]. One particular phenomenon—particle-size-dependent melting point depression—occurs when the particle size is of the order of nanometers, as first demonstrated by Takagi [2] by means of transmission electron microscope (TEM) observation. At these reduced dimensions, the surface-to-volume ratio is high and the surface energy substantially effects the interior "bulk" properties of the material. For example, the melting point T_m of nanometer-sized Au particles can be 300 K lower than the bulk value [3].

There are several phenomenological models [3–6] addressing the melting point depression of small metal particles. However, to facilitate a more comprehensive understanding of the thermodynamics of finite material systems, it is imperative to investigate experimentally the details of heat exchange during the melting process, in particular the latent heat of fusion ΔH_m . Recently, computational simulation work in Au clusters [7] has predicted a cluster-dependent depression of ΔH_m , in addition to the depression of T_m .

TEM is a standard technique for studying the size-dependent melting point depression phenomenon of small metal particles formed by thermal evaporation. At the melting point there are changes in the diffraction pattern associated with the disordering of the structure [2,3]. However, as particle size decreases the diffraction technique becomes increasingly inaccurate due to line broadening. Moreover, TEM is limited to structural measurement only; it cannot measure the heat associated with the melting process.

The ideal experimental technique for measuring melting of small particles is *calorimetry*. In addition to measuring T_m , it can measure the integral amount and the dynamics of the heat exchange. Until now, calorimetry has not been attempted for systems of nanometer dimension independently formed from deposition [8,9], due to the difficulty in measuring the minuscule amount of heat involved in these cases. For example, the energy con-

sumed during the melting of a 5 nm thick layer of Sn is equivalent to $\sim 1/10$ of the chemisorption energy of 1 monolayer of gas molecules on a crystal surface (e.g., O₂ on W surface). The energy is too small to be measured using existing differential scanning calorimetry.

The nanocalorimetric technique, however, can be much more sensitive by taking advantage of the advanced thin-film and membrane fabrication technology, in that the thermal mass of the calorimeter is dramatically reduced [10,11]. With its high sensitivity, nanocalorimetry also offers a potential to measure the premelting of particle surface quantitatively, so as to provide more detailed information for us to understand the entire solid-liquid transition in finite systems. And by measuring the specific heat capacity of the sample, we can obtain an accurate value for the total amount of material deposited.

In this Letter we present the first calorimetry measurements of the melting process of nanometer-sized Sn particles formed via thermal evaporation. The size-dependent melting point depression has been observed, and, for the first time, values for the latent heat of fusion ΔH_m have been obtained, which show that ΔH_m as well as T_m is particle size dependent.

Nanocalorimetric measurements were made by using our improved ultrafast scanning calorimetric technique [10]. Sn particles with radii ranging from 50 to 500 Å were formed by successive depositions (~ 3 Å/s) of pure Sn onto the SiN side of the thin-film calorimeter using the thermal evaporation process at pressures of $\sim 8 \times 10^{-8}$ Torr. For the small amounts of Sn deposited here, the films are discontinuous and form self-assembled nanometer-sized islands on the inert substrate. In contrast to embedding metal particles in bulk matrix [8,9], this type of sample preparation produces spherical Sn particles with high purity and free surfaces, which are ideal for studies of melting of small metal particles.

Calorimetric measurements were performed immediately after each deposition at a base pressure of $\sim 1 \times 10^{-8}$ Torr. Sn was also deposited on adjacent 3 mm Cu grids coated with 200 Å of amorphous carbon films for

TEM analysis. The particle size was measured using a Hitachi-S800 scanning electron microscope and a Phillips CM-12 TEM. An example of the particle size distribution is shown in the histogram of Fig. 1, which exhibits roughly a Gaussian distribution. The mean radius \bar{r} is hereafter taken as the Sn particle size. The average Sn particle size increases linearly with increasing the total amount of Sn deposited. For thinner samples where $\bar{r} < 80 \text{ \AA}$, the values for \bar{r} were obtained by extrapolation. Values for the total amount of Sn deposited, as determined by the increase of heat capacity of the calorimeter, agreed well ($\pm 7\%$) with values obtained with the crystal monitor.

The calorimetry measurement was initiated by applying a single, $\sim 10 \text{ ms}$ dc electrical pulse to the Ni thin-film heater, thus raising the temperature of the system (Ni heater, SiN membrane, and Sn sample) by Joule heating, as described in our previous work [10,12]. The current and voltage supplied to the heater were monitored in real time. Subsequent analysis of the change in the resistance of the Ni heater as a function of time provides accurate values for both the temperature of the system and the total amount of heat supplied to the system. As Sn particles melt, there is an abrupt change in the increasing rate of temperature, which is directly attributed to the fact that additional heat is needed for melting of Sn. In order to separate this amount of heat associated with melting from the total heat taken by the system, we subtract the heat attributed to the heat capacity of the system prior to the melting of Sn from the

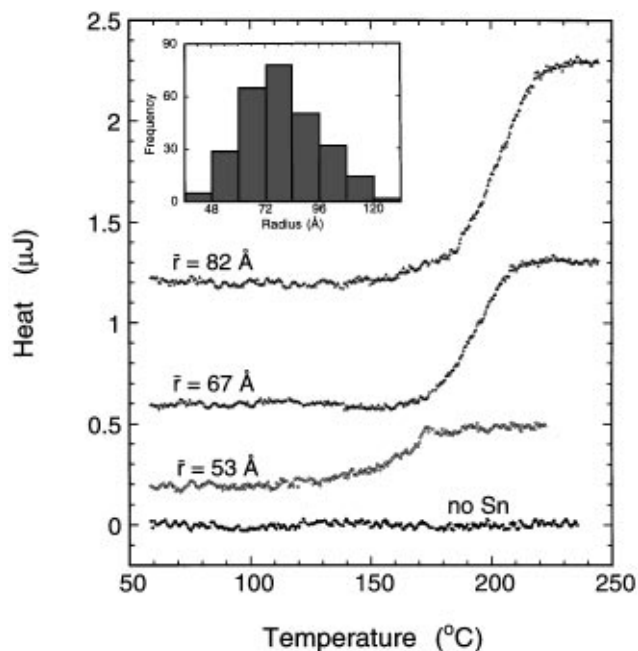


FIG. 1. The amounts of heat measured by calorimetry during the melting process for Sn particles of 53, 67, and 82 \AA in radii, respectively. The heat attributed to the average heat capacity of the entire system is subtracted from the total heat measured. The inset is a histogram of size distribution of Sn particles when $\bar{r} = 82 \text{ \AA}$. Each curve is offset for clarity.

total heat. The results are shown in Fig. 1. The abrupt "jump" in each curve is the signature of melting. The height of the jump is a measure of ΔH_m , the amount of heat required for melting, and as expected it decreases as the integral amount of Sn decreases. There is a broadening of the temperature range for melting, which is attributed to the size distribution of Sn particles as discussed later. The average melting point is defined as the temperature corresponding to the half-maximum of jump. Figure 1 clearly shows that the melting point decreases as the size of Sn particles decreases.

The size dependence of the average melting temperature and normalized heat of fusion is plotted in Fig. 2. For bulk Sn, the melting point is 232 $^{\circ}\text{C}$ [13]. It is evident that the melting points systematically decrease as the size of Sn particles decreases, a reduction of about 70 $^{\circ}\text{C}$ for Sn particles with $\bar{r} \approx 50 \text{ \AA}$. This phenomenon has also been observed by Wronski [14]. The depression of the melting temperature was confirmed during the course of this work by using TEM diffraction techniques during *in situ* heating of the Sn samples deposited on amorphous carbon films.

Surprisingly, the normalized heat of fusion ΔH_m also decreases markedly from the bulk value which is 58.9 J/g

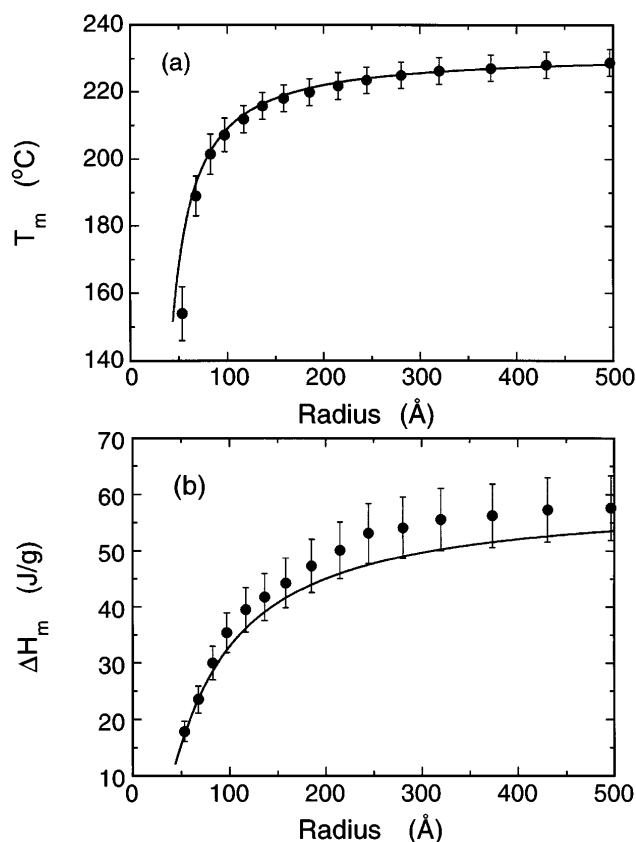


FIG. 2. (a) Size dependence of the melting points of Sn particles. The solid line is calculated in terms of Eq. (2). (b) Size dependence of the normalized heat of fusion. The solid is calculated in terms of Eq. (4).

[13] by as much as 70% when the particle size is reduced [Fig. 2(b)]. From the viewpoint of classical thermodynamics, the latent heat of fusion assumes a constant value. Not until recently have molecular-dynamics simulations shown a steady decrease of ΔH_m with decreasing cluster size for Au clusters [7].

To probe further the relationship between the particle size and T_m and ΔH_m , calorimetric measurements were made for a fixed amount of Sn by applying multiple dc current pulses to the calorimeter. T_m and ΔH_m were measured for each heating cycle, while particle size was measured as-deposited and after a series of heating cycles were done. Measurements revealed that both T_m and ΔH_m increased slightly with heating cycles and the particle size increased too, as expected due to coalescence.

Hansen [6] analyzed the melting temperature in terms of classical thermodynamics. The model assumes that a solid particle is embedded in a thin liquid overlayer and the melting temperature is taken to be the temperature of equilibrium between the solid sphere core and the liquid overlayer of a given critical thickness t_0 . t_0 is an adjustable parameter in accordance with the experimental results. Accordingly, the melting point T_m of Sn particles with radius r is expressed as

$$T_0 - T_m = \frac{2T_0}{\Delta H_0} \left[\frac{\sigma_s}{\rho_s(r - t_0)} + \left(\frac{\sigma_l}{r} + \frac{\Delta P}{2} \right) \times \left(\frac{1}{\rho_s} - \frac{1}{\rho_l} \right) \right], \quad (1)$$

where T_0 is the bulk melting temperature of solid Sn and ΔH_0 its latent heat of fusion, σ_s and σ_l are the interfacial surface tensions between the solid and the liquid and between the liquid and its vapor, respectively, and ρ_s and ρ_l are the densities of the solid and liquid, respectively, and t_0 is the critical thickness of the liquid layer at T_m . ΔP is the difference between the vapor pressure at the surface of the liquid layer with an outer radius r at T_m and the vapor pressure at flat liquid surface ($r = \infty$) at T_0 . It has been shown that ΔP can be neglected for Sn [14]. Substituting $T_0 = 232$ °C, $\rho_s = 7.18$ g/cm³, $\rho_l = 6.98$ g/cm³ [14], and $\sigma_l = 550$ mN/m [15] into Eq. (1), we obtain the following expression:

$$T_m = 232 - 782 \left[\frac{\sigma_s}{15.8(r - t_0)} - \frac{1}{r} \right], \quad (2)$$

where T_m is in °C and r and t_0 are in Å. The interfacial surface tension between the solid and liquid, σ_s , can be determined experimentally in terms of Eq. (2). The slope $dT_m/d(1/r)$ at large r is related to σ_s . From our measurement, σ_s is determined to be 48 ± 8 mN/m, which agrees with the values obtained by Turnbull [16] ($\sigma_s = 54.5$ mN/m) and Wronski [14] ($\sigma_s = 62.2 \pm 10$ mN/m).

By adjusting the value of the critical liquid layer thickness, we obtain a best fit to the experimental data in terms in Eq. (2) when $t_0 = 18$ Å [see Fig. 2(a)].

Recently, Kofman *et al.* [17] demonstrated the existence of a liquid layer on a nanometric Pb particle surface prior to complete melting by optical methods. In addition, computational simulations have also shown the liquidlike precursor prior to the complete melting of small Au particles [7].

The formation of a molten surface overlayer equilibrating with the solid core is directly related to the surface melting phenomenon. For example, the Pb(110) [18] and Al(110) [19] surfaces of bulk crystals have been observed to melt at temperatures below the bulk melting temperatures, with a continuous increase in the thickness of the melted layer as temperature approaches the bulk melting point. For small metal particles, the surface melting is strongly enhanced by curvature effects. Observations on Ni clusters [20] and Pb nanometric particles [21] show that the surface melting of small clusters or particles proceeds over a broader temperature range and that the thickness of the liquid layer is much larger than that observed on bulk crystals. For example, for Pb particles having a radius of 200 Å, the surface melting initiates about 100 °C below the melting temperature T_m , and the maximum thickness of the liquid layer can be as much as 40 Å [17].

In order to relate the heat of fusion to the heat measured by the calorimeter, we must consider the details of the melting process. Surface melting of small particles occurs in a continuous manner over a broad temperature range, whereas the homogeneous melting of the solid core occurs abruptly at the critical temperature T_m [21]. The total heat required for both surface and solid core melting is supplied by the calorimeter. However, the heat for the surface melting is supplied over a broad temperature range and appears as a gradual increase ($\sim 0.1\%$) in the background heat capacity of the system, a value which is too small to be measured by our present techniques. Conversely, the heat supplied for the abrupt melting of a solid core is directly measured using our technique.

In order to quantitatively describe the heat of fusion for small Sn particles, it is necessary to separate the volume of the liquid surface layer and the solid core region. We thus define the volume of the spherical liquid shell as an "excluded volume" δV in terms of the critical thickness t_0 of the liquid layer,

$$\delta V = \frac{4}{3} \pi [r^3 - (r - t_0)^3]. \quad (3)$$

Assuming that the latent heat of fusion per volume of the bulklike solid core is independent of temperature, we obtain the expression for the normalized heat of fusion in terms of the original particle size r , as shown in the following equation:

$$\Delta H_m = \Delta H_0 \left(1 - \frac{t_0}{r} \right)^3. \quad (4)$$

In Fig. 3, a plot of $(\Delta H_m/\Delta H_0)$ vs $1/r$ is shown. The solid line in the plot was determined by finding the best fit for the data using t_0 as the fitting parameter.

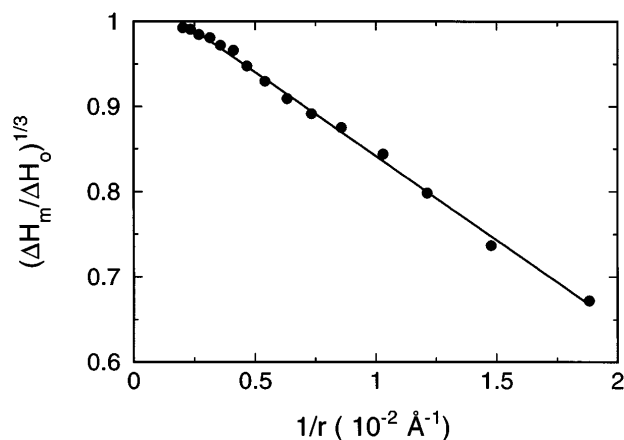


FIG. 3. Normalized heat of fusion as a function of the size of Sn particles. The solid line is generated using a model [Eq. (4)] which incorporates an excluded volume of the liquid region at the surface of the particles.

In this case we obtain a value of $t_0 \approx 16 \text{ \AA}$ for the thickness of the liquid layer, which agrees well with the value obtained from the melting point data ($t_0 \approx 18 \text{ \AA}$), as is shown in Fig. 2(a). These values for t_0 are obtained independently of each other. The deviation of the experimental data at large r from the straight line indicates that the thickness of the critical liquid layer is size dependent [17]. From Eq. (4), ΔH_m vanishes at the critical radius $r^* \sim 16 \text{ \AA}$. This sets a lower limit for the particle size at which bulk melting can be defined in terms of classical thermodynamics.

In summary, we have explored the size-dependent effects of heat of fusion and melting temperature of Sn particles with radii ranging from 50 to 500 \AA with a very sensitive scanning nanocalorimetric technique. The particle size dependence of the normalized heat of fusion is evident, and interpreted as a solid core melting following the gradual surface melting for small particles. An excluded volume of a solid particle is introduced to describe the latent heat of fusion quantitatively. In addition, the lowering of melting points with decreasing Sn particle size has been observed and is shown to agree with the results of others.

We gratefully acknowledge P. Infante of the National Nanofabrication Facility at Cornell University for the technical assistance in the fabrication of nanocalorimeters. Thanks are also due to Professor D. Cahill and Professor G. Ehrlich at University of Illinois at Urbana-Champaign for helpful discussions and critical reading of the manuscript. This work is financially supported by National Science Foundation (SGER DMR 94-19604) and the Joint

Services Electronics Program (JSEP, N00014-90-1-129). Microanalysis characterization was performed at the Center for Microanalysis, University of Illinois, supported by Department of Energy Grant No. DEFG 02-91ER35439.

- [1] K.N. Tu, J.W. Mayer, and L.C. Feldman, *Electronic Thin Film for Electrical Engineers and Material Scientists* (Macmillan, New York, 1992).
- [2] M. Takagi, *J. Phys. Soc. Jpn.* **9**, 359 (1954).
- [3] Ph. Buffat and J.-P. Borel, *Phys. Rev. A* **13**, 2287 (1976).
- [4] P. Pawlow, *Z. Phys. Chem.* **65**, 1 (1909); **65**, 545 (1909).
- [5] H. Reiss and I.B. Wilson, *J. Colloid Sci.* **3**, 551 (1948).
- [6] K.-J. Hanszen, *Z. Phys.* **157**, 523 (1960).
- [7] F. Ercolessi, W. Andreoni, and E. Tosatti, *Phys. Rev. Lett.* **66**, 911 (1991); H.S. Lim, C.K. Ong, and E. Ercolessi, *Z. Phys. D* **26**, S45 (1993).
- [8] K.M. Unruh, B.M. Patterson, and S.I. Shah, *J. Mater. Res.* **7**, 214 (1992); K.M. Unruh, T.E. Huber, and C.A. Huber, *Phys. Rev. B* **48**, 9021 (1993).
- [9] C.C. Koch, J.S.C. Jang, and S.S. Gross, *J. Mater. Res.* **4**, 557 (1989); J.S.C. Jang and C.C. Koch, *ibid.* **5**, 325 (1990).
- [10] S.L. Lai, G. Ramanath, L.H. Allen, P. Infante, and Z. Ma, *Appl. Phys. Lett.* **67**, 1229 (1995).
- [11] D.W. Denlinger, E.N. Abarra, K. Allen, P.W. Rooney, M.T. Messer, S.K. Watson, and F. Hellman, *Rev. Sci. Instrum.* **65**, 946 (1994).
- [12] L.H. Allen, G. Ramanath, S.L. Lai, and Z. Ma, *Appl. Phys. Lett.* **64**, 417 (1994).
- [13] *American Institute of Physics Handbook* (McGraw-Hill, New York, 1972), 3rd ed., pp. 4–243.
- [14] C.R.M. Wronski, *Br. J. Appl. Phys.* **18**, 1731 (1967). However, miscalculations might have occurred in obtaining Eq. (3). Such an equation has been rederived in this Letter as Eq. (2).
- [15] M.A. Carroll and M.E. Warwick, *Mater. Sci. Technol.* **3**, 1402 (1983).
- [16] D. Turnbull, *J. Appl. Phys.* **21**, 1022 (1955).
- [17] Y. Lereah, G. Deutscher, P. Cheyssac, and R. Kofman, *Europhys. Lett.* **12**, 709 (1990); P. Kofman, P. Cheyssac, A. Aouaj, Y. Lereah, G. Deutscher, T. Ben-David, J.M. Penisson, and A. Bourret, *Surf. Sci.* **303**, 231 (1994).
- [18] J.W.M. Frenken and J.F. van der Veen, *Phys. Rev. Lett.* **54**, 134 (1985); B. Pluis, T.N. Taylor, D. Frenkel, and J.F. van der Veen, *Phys. Rev. B* **40**, 1353 (1989).
- [19] A.W. Denier van der Gon, R.J. Smith, J.M. Gay, D.J. O'Connor, and J.F. van der Veen, *Surf. Sci.* **227**, 143 (1990); P. Stoltze, J.K. Nørskov, and U. Landman, *Phys. Rev. Lett.* **61**, 440 (1988).
- [20] Z.B. Güvenç and J. Jellinek, *Z. Phys. D* **26**, 304 (1993).
- [21] R. Garrigos, P. Cheyssac, and R. Kofman, *Z. Phys. D* **12**, 497 (1989).